JOURNAL OF MATERIALS SCIENCE 28 (1993) 5831–5835

Irreversible enthalpy relaxation of amorphous $(Fe_{1-x}Ni_x)_{83}P_{17}$ (x=0–1) alloys

T. H. NOH*, A. INOUE, H. FUJIMORI, T. MASUMOTO
Institute for Materials Research, Tohoku University, Sendai 980, Japan

This paper deals with the changes in exothermic enthalpy relaxation behaviour and Curie temperature of amorphous $Fe_{33}Ni_{50}P_{17}$ alloy upon annealing, and the compositional effect (i.e. the change with Fe/Ni ratio) on the magnitude of exothermic reactions during continuous heating of $(Fe_{1-x}Ni_x)_{83}P_{17}$ ($x = 0$–1) alloys, in order to clarify the thermal relaxation behaviour with irreversibility of metal–metalloid type amorphous alloys. For $Fe_{33}Ni_{50}P_{17}$ alloy, the exothermic reaction showed two distinctive peaks at about 480 and 580 K and the low-temperature peak had a very strong correlation with the change in Curie temperature. Furthermore it was observed that for $(Fe_{1-x}Ni_x)_{83}P_{17}$ alloys the magnitude of the low-temperature peak was nearly proportional to the number of Fe–Ni atom pairs. However, the high-temperature one was almost independent of the changes in Curie temperature and the ratio of Fe to Ni. These results suggest that the exothermic enthalpy relaxation peak at temperatures far below T_g (or T_x) originates from the local rearrangement of metal–metal interactions of different species, while the high-temperature peak is due to the rearrangement of metal–metalloid bonding. This separation into two stages is interpreted as due to the difference of bonding forces between metal–metal and metal–metalloid pairs in amorphous Fe–Ni–P alloys.

1. Introduction

Structural relaxation is one of the main research subjects for non-equilibrium amorphous alloys with respect to scientific and practical interest. Up to now, various physical characteristics such as Curie temperature [1, 2], internal friction [3, 4], electrical resistivity [5, 6], magnetic anisotropy [7, 8] and Young's modulus [9, 10] have been measured with the aim of clarifying the relaxation phenomenon.

For many physical properties, it is known that specific heat measurement is a good means of examining the structural relaxation phenomenon. Furthermore, it has been clarified that in compliance with the structural relaxation, the specific heat changes reversibly and irreversibly through endothermic and exothermic reactions, respectively.

Recently, with the analysis of reversible endothermic enthalpy relaxation behaviour, Inoue *et al.* [11, 12] proposed that there exist two stages of structural relaxation for many metal–metalloid type amorphous alloys, i.e. (i) the local rearrangement of metal–metal atom pairs at low temperatures well below T_g and (ii) the long-range regroupings of metal–metalloid atom pairs at high temperatures near T_g. Although a number of reports on exothermic enthalpy relaxation have been made [13, 14] and as a result the presence of two distinctive relaxation spectra has been proposed, a more systematic study on the inherent nature of exothermic reaction is required because of the importance of this problem for non-equilibrium amorphous alloys.

In this paper, the relationship between exothermic enthalpy relaxation and the change in Curie temperature indicative of chemical short-range ordering, and the compositional effect on the magnitude of exothermic reaction, were investigated in order to understand the details of exothermic reactions of amorphous alloys in the framework of a two-stage enthalpy relaxation mechanism.

2. Experimental procedure

Various $(Fe_{1-x}Ni_x)_{83}P_{17}$ ($x = 0$–1) amorphous alloys were prepared in the form of ribbon of about 20 μm thick and 1.0 mm wide by the single-roller melt-spinning method. The samples were confirmed to be amorphous by conventional X-ray diffraction using CuK_α radiation.

The apparent specific heat (C_p) and Curie temperature (T_C) were measured with a differential scanning calorimeter (Perkin-Elmer DSC II). For $Fe_{33}Ni_{50}P_{17}$ alloy, the as-quenched samples were annealed at various temperatures below the glass transition temperature T_g (T_a = 400–600 K) for t_a = 60 s. The annealing time (t_a) was chosen to avoid the appearance of a reversible endothermic peak. All the annealing treatments of the encapsulated samples were performed directly inside the calorimeter and the heating and

Present address: Korea Institute of Science and Technology, Seoul 136-791, Korea.

0022–2461

cooling rates were 5.33 K s^{-1}. Following the annealing treatment, the samples were thermally scanned at 0.67 K s^{-1} from 320 to 645 K to determine $C_{p,a}$, the specific heat of the annealed sample. They were then cooled to 320 K, and reheated immediately to obtain the C_p data of the stabilized reference samples ($C_{p,s}$). The change in the calorimetric behaviour with annealing was used to monitor the structural relaxation processes. The accuracy of the data was about 0.8 J mol^{-1} K^{-1} for the absolute C_p values, and was better than 0.2 J mol^{-1} K^{-1} for the relative C_p or ΔC_p measurements.

The measurement procedure of C_p data for all the as-quenched $(Fe_{1-x}Ni_x)_{83}P_{17}$ alloy samples was the same as that for annealed $Fe_{33}Ni_{50}P_{17}$. The highest heating temperature used to obtain the specific heat of an as-quenched sample was about 20 K lower than the crystallization temperature (T_x).

3. Results and discussion

3.1. Exothermic enthalpy relaxation behaviour and change in T_C of as-quenched and annealed $Fe_{33}Ni_{50}P_{17}$ alloy

Fig. 1 shows the specific heat as a function of temperature for as-quenched and annealed $Fe_{33}Ni_{50}P_{17}$ amorphous alloy. With heating of the as-quenched sample the specific heat decreases gradually, and then rapidly increases in the glass transition range. As mentioned earlier, $C_{p,s}$ is the specific heat of the fully relaxed samples. The difference between $C_{p,q}$ and $C_{p,s}$ is caused by exothermic reactions inducing irreversible enthalpy relaxation. In Fig. 2, the temperature dependence of the exothermic reaction ($\Delta C_p(T) = C_{p,s} - C_{p,q}$) is shown, and the total reaction is estimated to be 1.28 kJ mol^{-1}.

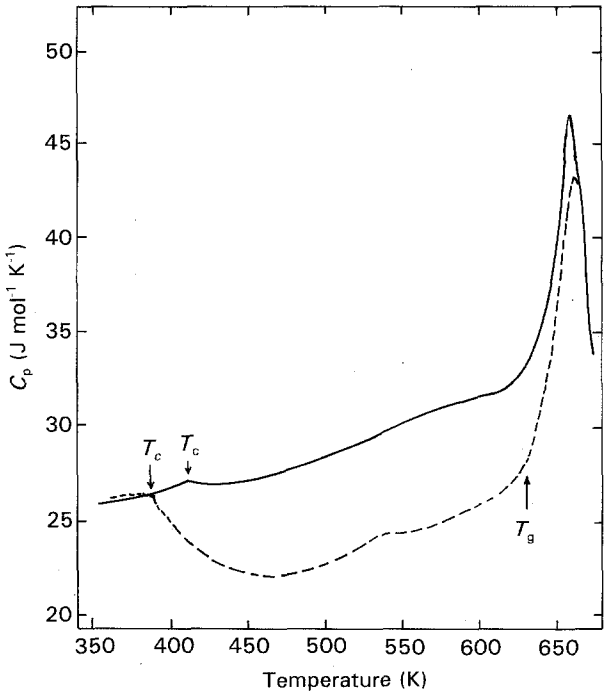

Figure 1 Thermograms of (- - -) an amorphous $Fe_{33}Ni_{50}P_{17}$ alloy in the as-quenched state ($C_{p,q}$) and (—) the sample subjected to heating to 640 K ($C_{p,s}$). Heating rate 0.67 K s^{-1}.

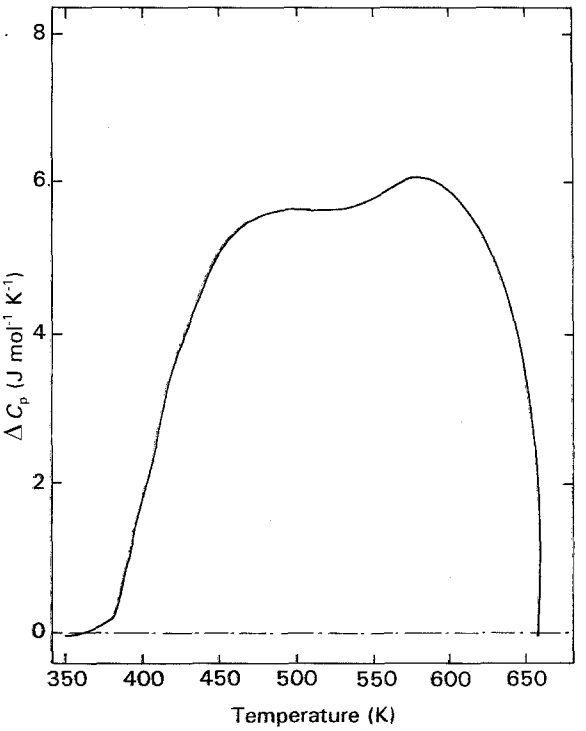

Figure 2 Difference between $C_{p,s}$ and $C_{p,q}$ ($= \Delta C_p$(exo)) plotted against temperature for an amorphous $Fe_{33}Ni_{50}P_{17}$ alloy. Heating rate 0.67 K s^{-1}; $\Delta H_{exo} = 1.28$ kJ mol^{-1}.

Fig. 3 shows the apparent specific heat $C_{p,a}$ of amorphous $Fe_{33}Ni_{50}P_{17}$ alloy samples subjected to isochronal annealing treatments at various temperatures for $t_a = 60$ s. The specific heat of the as-quenched sample, $C_{p,q}$, is also shown for comparison. The magnitude of anneal-induced exothermic enthalpy relaxation, ΔH_{exo}, is determined from the data of $C_{p,a}$ and $C_{p,q}$ by the relation

$$\Delta H_{exo} = \int (C_{p,a} - C_{p,q})\, dT$$

As shown in Fig. 3, when T_a rises the $C_{p,a}$ curves shift to the higher-temperature side. Fig. 4 shows the ΔC_p spectra corresponding to the difference of C_p values between the stabilized reference sample and the as-quenched or annealed sample. The ΔC_p curve consists of two distinct peaks centred at about 480 K and 580 K respectively, indicating the existence of two distinguishable relaxation stages.

A relaxation process with an activation energy Q has a time constant given by $\tau = \tau_o \exp(Q/kT)$ where τ_o is a characteristic time constant. If annealed at T_a for t_a, the processes whose time constants τ are less than t_a, i.e. processes with activation energies up to $Q = kT \ln(\nu_o t_a)$ where ν_o is a characteristic vibration frequency, will be relaxed. If the vibration frequency is assumed to be the Debye frequency ($\sim 10^{13}$ s^{-1}), the activation energy for the low-temperature relaxation process is approximated to be 1.1–1.4 eV and that of the high-temperature relaxation is 1.5–1.8 eV from the above equations. However, in the case of the cooperative relaxation process at high temperature near T_g, the entropy term $\exp(S/k)$ where S and k are the activation entropy and Boltzmann constant, respectively, must be considered in the evaluation of the characteristic frequency constant [15]. This consid-

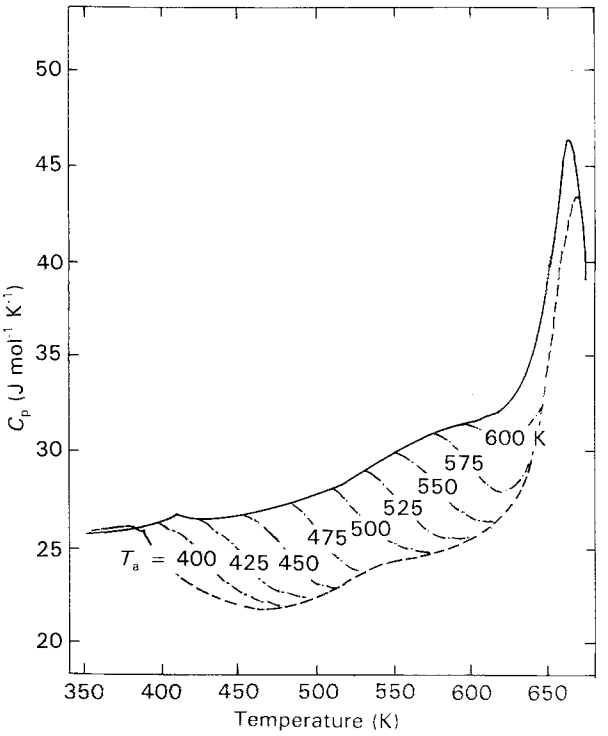

Figure 3 Thermograms of (---) an amorphous $Fe_{33}Ni_{50}P_{17}$ alloy annealed for 60 s at various temperatures from 400 to 600 K ($C_{p,a}$), (—) the as-quenched sample ($C_{p,s}$) and (- - -) the sample subjected to heating to 640 K ($C_{p,q}$). Heating rate 0.67 K s^{-1}.

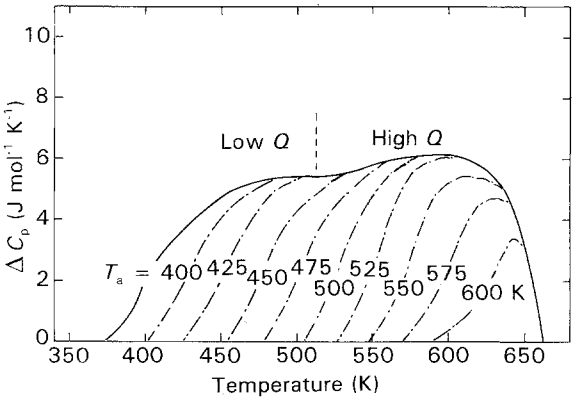

Figure 4 Difference between $C_{p,a}$ (or $C_{p,q}$) and $C_{p,s}$ plotted against temperature for an amorphous $Fe_{33}Ni_{50}P_{17}$ alloy. t_a = 60 s, heating rate 0.67 K s^{-1}.

eration then brings about higher vibration frequencies and consequently larger activation energies than the Q values estimated above.

In Fig. 5, both the anneal-induced exothermic enthalpy relaxation (ΔH_{exo}) and the corresponding change of Curie temperature are given to obtain more detailed information on the two-stage enthalpy relaxation seen in Fig. 4. Annealing treatment below T_a = 450 K results in a marked increase in T_C. Although the anneal-induced exothermic enthalpy increases almost linearly with increasing T_a in the range above 450 K, the alteration of T_C is diminished and becomes constant above T_a = 550 K. From these results one can deduce the following two points; (i) at T_a below 450 K, chemical short-range ordering responsible for a change in T_C is the dominant relaxation

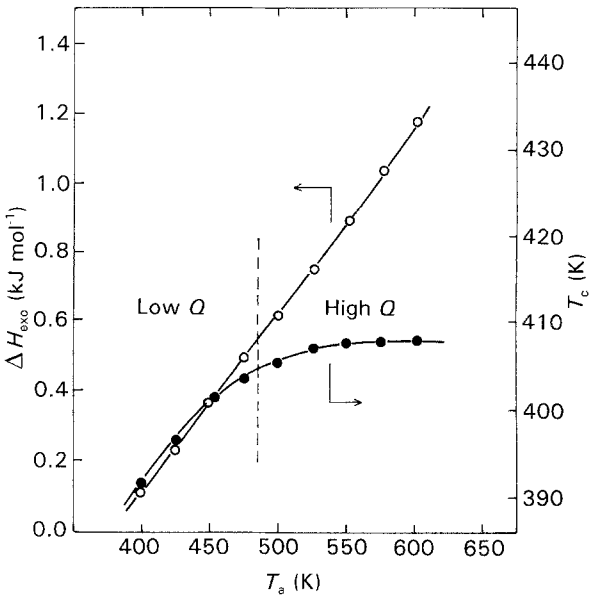

Figure 5 Variations of the anneal-induced exothermic heat (ΔH_{exo}) and the Curie temperature (T_C) as a function of annealing temperature for an amorphous $Fe_{33}Ni_{50}P_{17}$ alloy annealed for 60 s at various temperatures from 400 to 600 K.

process, and (ii) the contribution of this process to the anneal-induced enthalpy relaxation decreases in the range of T_a above 450 K. It is strongly believed [16] that chemical short-range ordering of different magnetic atoms in Fe–Ni base amorphous alloys is the main origin of the change in T_C at low temperatures well below T_g. Therefore it is most likely that the low-temperature peak in Fig. 4 resulted from localized metal–metal interactions, i.e. rearrangement between Fe and Ni atoms. However, in order to further clarify the role of Fe–Ni interaction in the exothermic reaction, an extensive study of the compositional effect is required.

3.2. Compositional dependence of exothermic enthalpy relaxation in $(Fe_{1-x}Ni_x)_{83}P_{17}$ alloys

In order to determine the effect of metal–metal (Fe–Ni) interaction on the low-temperature relaxation spectra, $\Delta C_p(T)$ ($= C_{p,s} - C_{p,q}$) curves of $(Fe_{1-x}Ni_x)_{83}P_{17}$ alloy samples with different ratios of Fe to Ni were examined.

As shown in Fig. 6, both the addition of Ni to binary Fe–P alloy and Fe to Ni–P binary alloy give rise to a prominent increase in the low-temperature relaxation spectra, and all the ΔC_p curves of Fe–Ni–P ternary alloys have peaks at a temperature of about 400–500 K and just below the crystallization temperature. The separation into two stages of exothermic enthalpy relaxation is attributed to the difference of kinetics resulting from different relaxation times between two reaction groups, and the occurrence of a low-temperature peak is ascribed to Fe–Ni interactions with short relaxation times. The experimental results and interpretation are also supported by the results of Veukel and Radelaar [17], in which, on the basis of activation energy spectra and a free volume

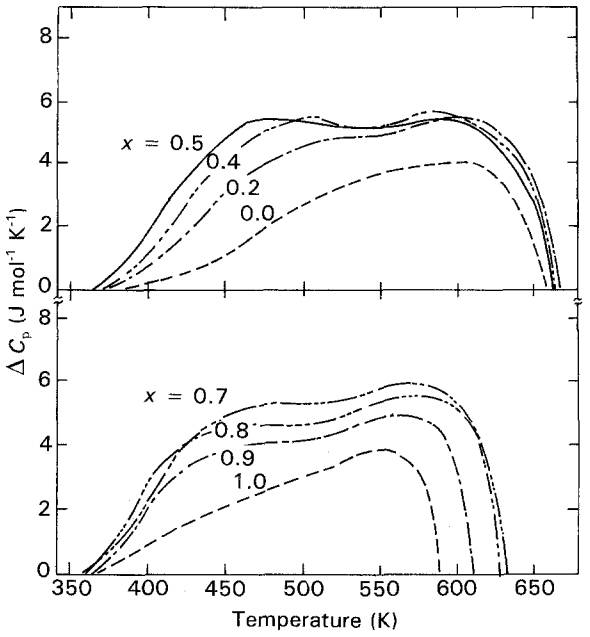

Figure 6 The difference between $C_{p,s}$ and $C_{p,q}$ plotted against temperature for amorphous $(Fe_{1-x}Ni_x)_{83}P_{17}$ ($x = 0$–1) alloys. Heating rate 0.67 K s^{-1}.

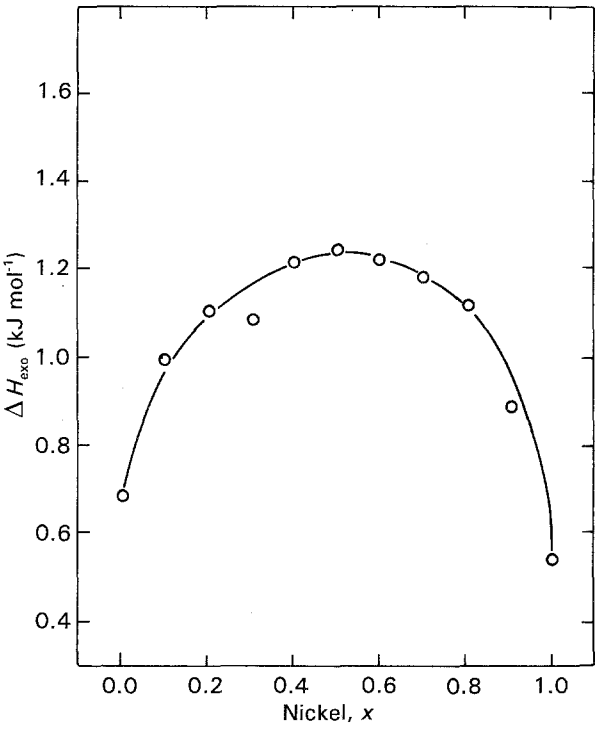

Figure 7 Variation of total exothermic heat upon continuous heating as a function of Ni content for amorphous $(Fe_{1-x}Ni_x)_{83}P_{17}$ ($x = 0$–1) alloys. The solid line is to guide the reader's eye.

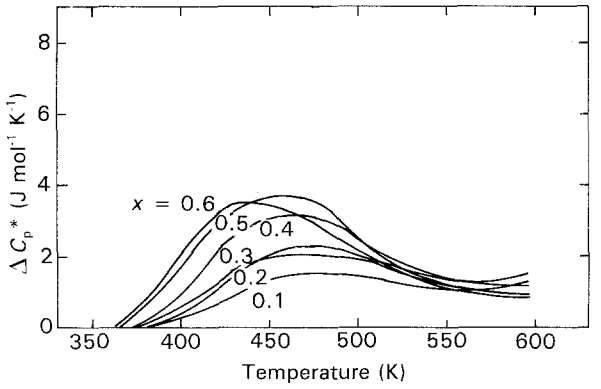

Figure 8 Differences in the exothermic reaction spectra between amorphous $(Fe_{1-x}Ni_x)_{83}P_{17}$ ($x = 0.1$–0.6) and $Fe_{83}P_{17}$ alloy plotted against temperature. Heating rate 0.67 K s^{-1}.

model, theoretical calculation of the ΔC_p curve yields two peaks and the first low-temperature peak corresponds to the maximum rate of chemical order change.

In the case of the high-temperature relaxation peak near T_g (or T_x) for Fe-rich alloy ($x \leq 0.6$), the magnitude of ΔC_p is nearly the same and independent of the alloy composition. On the other hand, the low-temperature relaxation shows a marked change with the ratio of Fe to Ni, as exemplified in Fig. 6. This implies that the high-temperature relaxation peak is due not to chemical ordering among metallic species but to a change of the topological structure of metal–metalloid (Fe–P, Ni–P) atoms. The large difference in the high-temperature relaxation peaks for the Ni-rich alloys is because of the significant decrease of T_x with increasing Ni content.

The total exothermic heat released upon continuous heating as a function of Ni content is shown in Fig. 7. The value exhibits a maximum at $x = 0.5$, i.e. equiatomic composition of the two metal atoms, suggesting that the heating-induced rearrangement of Fe and Ni atoms is most remarkable at $x = 0.5$.

In order to evaluate the effect of chemical ordering on the low-temperature exothermic enthalpy relaxation, the difference between the ΔC_p values of the ternary alloys with $x \leq 0.6$ and that of Fe–P binary alloy (ΔC_p^*) was obtained as plotted in Fig. 8, and was integrated to 550 K. The values thus obtained are plotted in Fig. 9 as a function of $x(1 - x)$, which is proportional to the total number of Fe–Ni atom pairs. There exists a fairly good linear relationship between the magnitude of the low-temperature exothermic enthalpy relaxation and the number of Fe–Ni atom pairs. This result is consistent with the interpretation described above, that the local rearrangement interaction between different metallic atoms gives rise to an exothermic enthalpy relaxation at temperatures well below T_g (or T_x) corresponding to the first peak of the ΔC_p curve.

4. Summary

In order to clarify the irreversible exothermic enthalpy relaxation behaviour of Fe–Ni–P amorphous alloys upon annealing, anneal-induced changes in exothermic reaction and Curie temperature of $Fe_{33}Ni_{50}P_{17}$ amorphous alloy were investigated by means of differential scanning calorimetry. Additionally, the exothermic reaction during continuous heating of $(Fe_{1-x}Ni_x)_{83}P_{17}$ amorphous alloys was measured as a function of the ratio of Fe to Ni.

For $Fe_{33}Ni_{50}P_{17}$ alloy, the exothermic enthalpy relaxation takes place in two stages with two distinct peaks at about 480 K and 580 K; the change in the

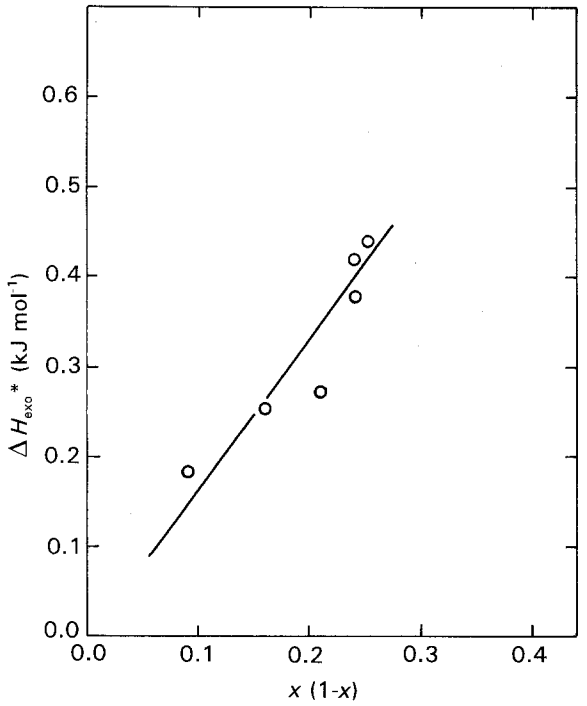

Figure 9 Relation between excess exothermic heat upon continuous heating and the factor $x(1-x)$ for amorphous $(Fe_{1-x}Ni_x)_{83}P_{17}$ ($x \leq 0.6$) alloys. The solid line represents the linear relationship between ΔH_{exo}* and the number of Fe–Ni neighbours.

first peak at 480 K has a strong correlation with that in T_C, indicating that the low-temperature relaxation is due to chemical ordering among Fe–Ni atoms.

Furthermore, from investigation of the compositional effect on the exothermic enthalpy relaxation of $(Fe_{1-x}Ni_x)_{83}P_{17}$ alloys, it was found that the magnitude of the exothermic reaction of the low-temperature peak is nearly proportional to the number of Fe–Ni bond pairs, and the high-temperature second peak is independent of changes in the ratio of Fe to Ni.

In conclusion, it is deduced that the low-temperature exothermic enthalpy relaxation peak is due to local metal–metal (Fe–Ni) interactions with low activation energies (about 1.1–1.4 eV), and the high-temperature exothermic enthalpy relaxation is due to the rearrangements of the metal–metalloid bond structure with higher activation energies. The separation of relaxation into two stages can be interpreted as due to the difference of bonding forces between metal–metal (Fe–Ni) and metal–metalloid (Fe–P, Ni–P) pairs.

References

1. H. S. CHEN, R. C. SHERWOOD, H. J. LEAMY and E. M. GYORGY, *IEEE Trans. Magn.* **MAG-12** (1976) 933.
2. Y. N. CHEN and T. EGAMI, *J. Appl. Phys.* **50** (1979) 7615.
3. B. S. BERRY and W. C. PRITCHET, *ibid.* **44** (1973) 3122.
4. N. MORITO and T. EGAMI, *J. Non-Cryst. Solids* **61/62** (1984) 973.
5. M. BALANZAT, *Scripta Metall.* **14** (1980) 173.
6. M. E. SONIUS, B. J. THIJSSE and A. van den BEUKEL, *ibid.* **17** (1983) 545.
7. F. E. LUBORSKY and J. L. WALTER, *IEEE Trans. Magn.* **MAG-13** (1977) 953.
8. W. CHAMBRON and A. CHAMBEROD, *Solid State Commun.* **33** (1980) 157.
9. A. KURSUMOVIC, M. G. SCOTT, E. GIRT and R. W. CHAN, *Scripta Metall.* **14** (1980) 1303.
10. A. L. MULDER, S. van der ZWAAG and A. van den BEUKEL, *J. Non-Cryst. Solids* **61/62** (1984) 969.
11. A. INOUE, T. MASUMOTO and H. S. CHEN, *J. Mater. Sci.* **19** (1984) 3953.
12. A. INOUE, H. S. CHEN and T. MASUMOTO, *ibid.* **20** (1985) 2417.
13. H. S. CHEN and E. COLEMAN, *Appl. Phys. Lett.* **28** (1976) 245.
14. P. G. ZIELINSKI and D. G. AST, *J. Non-Cryst. Solids* **61/62** (1984) 1021.
15. G. E. FISH, *IEEE Trans. Magn.* **MAG-21** (1985) 1996.
16. T. EGAMI, *ibid.* **MAG-17** (1981) 2600.
17. A. V. D. VEUKEL and S. RADELAAR, *Acta Metall.* **31** (1983) 419.

Received 1 July 1992
and accepted 27 April 1993